

Research Article

Simulation and Modeling of Flow in a Gas Compressor

Anna Avramenko,¹ Alexey Frolov,² and Jari Hämäläinen³

¹Centre of Computational Engineering and Integrated Design (CEID), Lappeenranta University of Technology, 53850 Lappeenranta, Finland

²Laboratory of Applied Mathematics and Mechanics, Saint Petersburg State Polytechnical University, Saint Petersburg 195251, Russia

³Lappeenranta University of Technology, 53850 Lappeenranta, Finland

Correspondence should be addressed to Anna Avramenko; anna.avramenko@lut.fi

Received 22 October 2014; Revised 16 December 2014; Accepted 24 December 2014

Academic Editor: Guan H. Yeoh

Copyright © 2015 Anna Avramenko et al. This is an open access article distributed under the Creative Commons Attribution License, which permits unrestricted use, distribution, and reproduction in any medium, provided the original work is properly cited.

The presented research demonstrates the results of a series of numerical simulations of gas flow through a single-stage centrifugal compressor with a vaneless diffuser. Numerical results were validated with experiments consisting of eight regimes with different mass flow rates. The steady-state and unsteady simulations were done in ANSYS FLUENT 13.0 and NUMECA FINE/TURBO 8.9.1 for one-period geometry due to periodicity of the problem. First-order discretization is insufficient due to strong dissipation effects. Results obtained with second-order discretization agree with the experiments for the steady-state case in the region of high mass flow rates. In the area of low mass flow rates, nonstationary effects significantly influence the flow leading stationary model to poor prediction. Therefore, the unsteady simulations were performed in the region of low mass flow rates. Results of calculation were compared with experimental data. The numerical simulation method in this paper can be used to predict compressor performance.

1. Introduction

Detailed experimental and numerical research of flow structures in centrifugal compressors began in the last century. Nonstationary effects were experimentally observed and described in detail in [1]. The issue of flow stall formation with impellers of open and closed types was investigated depending on the flow rate.

Eckardt (1976) [2], a classical work in the domain, considered impellers with high rotating speeds. The flow structure was compared with the numerical results and the flow separation was analyzed. The matter of using three-dimensional simulations of a viscous flow for design and analysis of centrifugal compressors was examined in [3]. Two different codes were used to obtain the results; they are compared to experimental data. However, both codes underestimated the appearance of pressure losses in the impeller.

Compressor Design Department of Saint Petersburg Polytechnical University has a special test stand for gas compressors. This stand allows the measurement of different instantaneous and mean parameters, such as pressure,

velocity, and temperature. The basic characteristic of gas compressors is the pressure characteristic that shows the dependence of the gas pressure ratio from mass flow rate for a given rotational speed.

The compressor under research is a laboratory low-pressure centrifugal compressor with a vaneless diffuser. It was designed for very low total pressure ratios ($\pi < 1.06$). This could lead to convergence issues. Moreover, the stalling regime was observed close to the efficiency point indicating that nonstationary effects were very strong in this compressor. Experimental studies of nonstationary phenomenon, called rotating stall, have been carried out. The rotating stall is a local instability in the flow realizing in disturbance of the circumferential flow pattern, reduction of the flow rate, and appearance of flow separation, resulting in the formation of rotated stall cells [4]. The number and rotational speed of the stall cells usually differ correspondingly from the number and rotational speed of compressor blades. Normally, the rotating stall happens at low mass flow rates.

Up to now, there were a small number of papers, known to authors, devoted to numerical simulation of the centrifugal

compressor [5–7] and numerical simulation of rotating stall effect [8, 9] but no papers with comparison of numerical results with physical experiments.

The objective of this work is a numerical simulation of the gas flow in the centrifugal compressor and validation of the obtained results against the physical experiment.

2. Description of the Problem

Experimental data and the geometry of a single-stage centrifugal compressor with a vaneless diffuser were provided by Compressor Design Department of Saint Petersburg State Polytechnical University. The experiments were carried out for eight regimes with different mass flow rates. Three different cross-sections of the compressor duct were examined during the experiments. These cross-sections are the inlet, diffuser inlet, and diffuser outlet (see Figure 1).

Tables 1-2 present the experimental data such as initial temperature (T_0), mass flow rate (G), atmospheric pressure (p_0) in the inlet, pressure ratio (π_1) at the diffuser inlet, and pressure ratio (π_2) at the diffuser outlet. Pressure ratio in the current section of the compressor is a ratio of the average absolute pressure in this section to the average absolute pressure in inlet.

The compressor contains 16 rotational blades. The rotating speed of the impeller is 6944 rpm. The diameter of the impeller is 275 mm (Figures 2 and 3).

Periodic boundary conditions are used when the flows across two opposite planes in a computational model are identical [10]. The current model illustrates a typical application of periodic boundary conditions. Here, the flow entering the computational model through one periodic plane is identical to the flow exiting the domain through the opposite periodic plane. Periodic planes are always used in pairs as illustrated in this example. So, only one part of geometry with one blade was studied.

Wall boundaries can be either stationary or moving. The stationary boundary condition specifies a fixed wall, whereas the moving boundary condition (e.g., using a moving reference frame) can be used to specify the translational or rotational velocity of the wall or the velocity components [10].

The boundary conditions for the studied model are shown in Figure 4.

3. Results

3.1. Numerical Setup and Results in NUMECA FINE/TURBO. Steady-state simulations were done in NUMECA FINE/TURBO 8.9.1 using different available turbulence models and discretization schemes. The calculations were carried out on a single structured mesh with 700 000 control volumes. The mesh was constructed to fit the wall y^+ values below 1 (boundary cell width 10^{-5} m).

Figures 5 and 6 show the pressure characteristic comparison for results obtained by first-order upwind discretization schemes for the Spalart-Allmaras turbulence model without and with wall functions, the $\kappa - \varepsilon$ model with wall functions, the shear-stress transport model without and with wall functions, and $v^2 - f$ model to experimental values. Pressure

TABLE 1: Experimental data for regimes 1–4.

Regimes	1	2	3	4
T_0 (K)	294.6	294.8	294.8	294.9
G (kg/s)	0.629	0.553	0.495	0.434
p_0 (Pa)	101791	101778	101778	101778
π_*^1	1.047	1.053	1.060	1.066
π_*^2	1.045	1.051	1.056	1.061

TABLE 2: Experimental data for regimes 5–8.

Regimes	5	6	7	8
T_0 (K)	295.0	295.0	295.1	295.2
G (kg/s)	0.312	0.266	0.116	0.105
p_0 (Pa)	101911	101765	101765	101765
π_*^1	1.073	1.076	1.076	1.075
π_*^2	1.068	1.069	1.068	1.067

characteristic is dependent on pressure ratio from mass flow rate with given rotational speed.

The first-order turbulence models give out similar results of pressure characteristic. As could be noticed from the figure, the calculated pressure characteristics are plain even where nonstationary effects are strong (below 0.3 kg/s). Moreover, the obtained total pressure ratio is within predicted values in the region of high mass flows. It could result in high pressure losses due to dissipation effect of first-order schemes. Therefore, the first-order approximation is insufficient to reproduce the stationary characteristic of the low-pressure ratio compressor.

Figures 7 and 8 show the pressure characteristic comparison for results obtained by second-order central discretization schemes for the Spalart-Allmaras turbulence model without wall functions to experimental values. There are strong convergence issues for low mass flow rates that could regard strong instabilities in the flow reproduced by the second-order discretization.

The conclusion could be that the second-order central discretization scheme conforms to the pressure characteristic shape much better than first-order upwind schemes. In addition, the pressure ratio does not conform to the experimental results in the region of high mass flows. Due to ignoring of hub and shroud leakages, the observed deviation of the pressure ratio was to be expected. In the region of low mass flow rates, nonstationary effects are dominant and steady-state simulations are not capable of capturing them.

Figures 9–12 show a large vortex structure (the rotating stall) formation with the mass flow rate decreasing from 0.5 kg/s to 0.175 kg/s. A strong difference between flow fields predicted by the first- and second-order discretization techniques is noticeable.

The large vortex structure starts to form when the flow rate falls below 0.4 kg/s only if the second-order scheme is used. First-order schemes do not predict any vortex structures until the flow rate falls below 0.2 kg/s, but even then predicted structures are not very large. This could be attributed to strong numerical dissipation effects that are

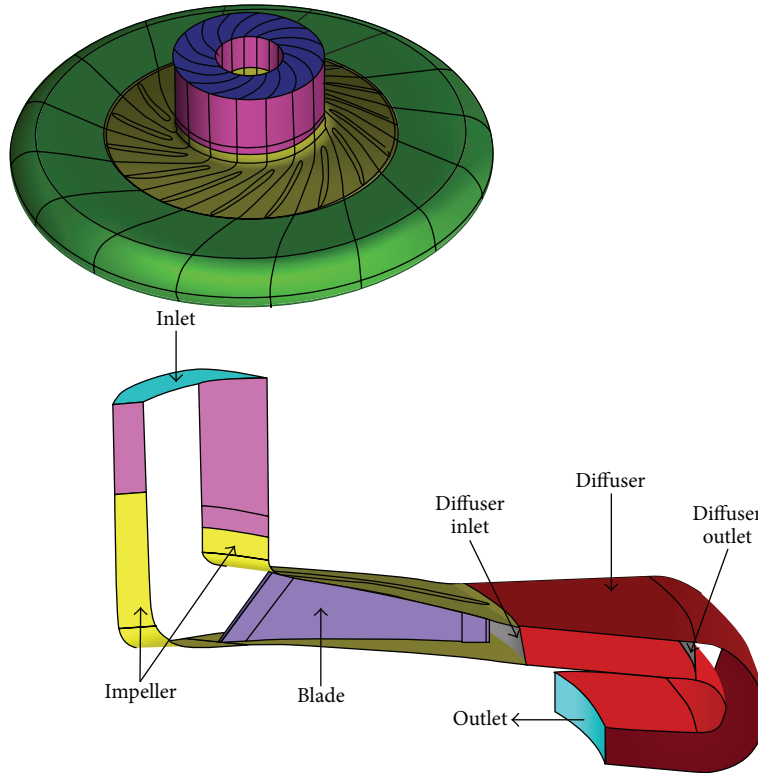


FIGURE 1: Geometry of the centrifugal compressor.



FIGURE 2: Geometry of the impeller.

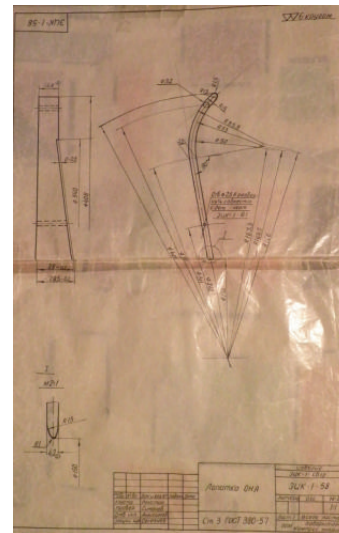


FIGURE 3: Geometry of the blade.

present when using first-order schemes. The stalling regime is very strong when using second-order central schemes. Due to strong influence of unsteady effects on mean flow parameters, unsteady simulations are needed to be carried out for accurate capturing of these effects.

3.2. Numerical Setup and Results in ANSYS FLUENT 13.0. Steady-state and unsteady simulations were done in ANSYS FLUENT 13.0 using the realizable $\kappa - \epsilon$ turbulence model with enhanced wall treatment [4]. Two different meshes are computed, namely, a coarse mesh containing 75 000 hexahedral elements and a refined mesh with 600 000 elements. The second-order upwind spatial discretization was used for the simulations. The results in the stationary case were obtained

for all regimes on the coarse mesh and for regimes 1–7 on the refined mesh.

Figures 13 and 14 show the pressure characteristics for the stationary case.

It is clear from the pressure characteristic that computed pressure ratio values are slightly over experimental curve. This could be attributed to neglecting the influence of hub and shroud leakages. The shape of the numerical characteristic

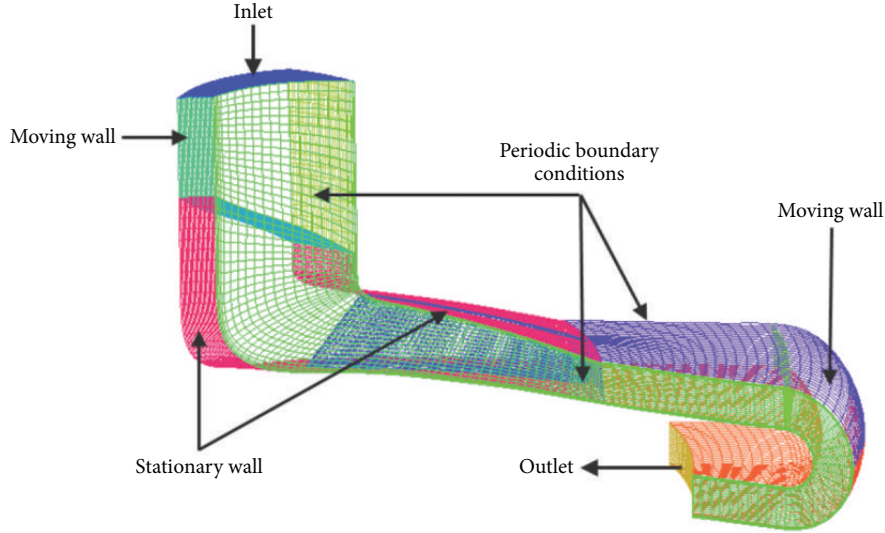


FIGURE 4: Boundary conditions.

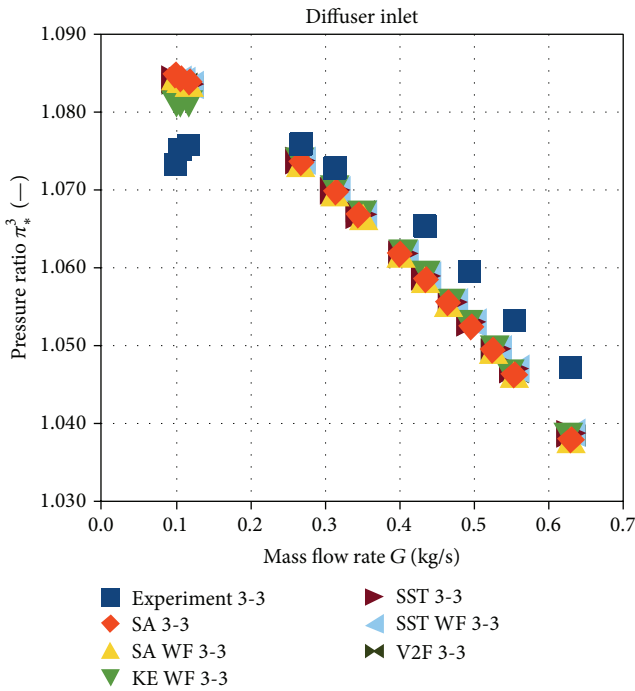


FIGURE 5: Pressure characteristic at the diffuser inlet for different turbulence models using first-order upwind discretization.

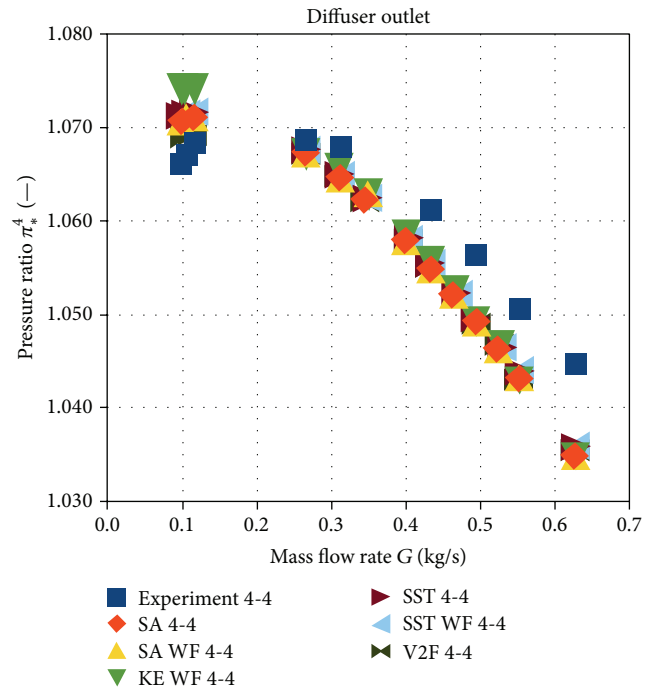


FIGURE 6: Pressure characteristic at the diffuser outlet for different turbulence models using first-order upwind discretization.

is in a good agreement with the shape of the experimental characteristic.

All nonstationary effects were observed in the experiments in the regimes with small mass flow rates. Therefore, only the first three regimes in the unsteady simulations were omitted.

Unsteady calculations were done in a transient formulation with first-order time discretization. 20 and 100 time steps for one period for the coarse and refined mesh were chosen,

respectively. Thus, the time step for the coarse mesh was equal to $2.7e - 05$ s (twenty iterations in the period) and $5.4e - 06$ s (one hundred iterations in the period) for the refined mesh.

The pressure characteristics for the unsteady case are shown in Figures 15 and 16.

As can be clearly seen from the figures, the unsteady pressure characteristics are very similar to stationary pressure characteristics.

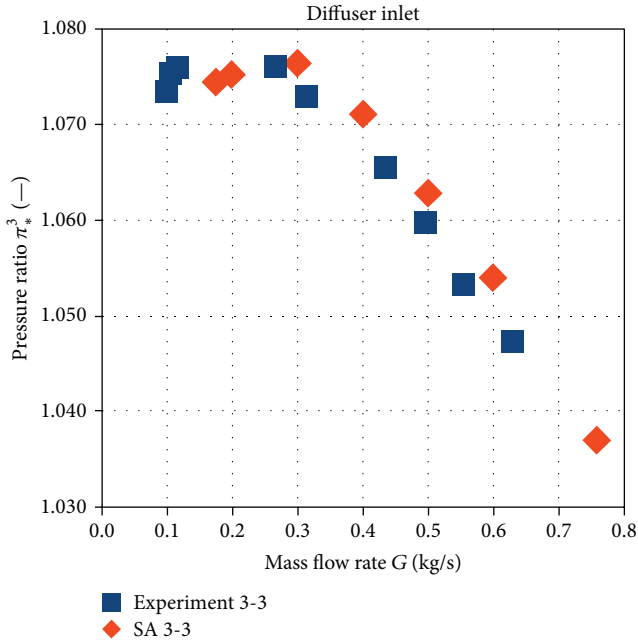


FIGURE 7: Pressure characteristic at the diffuser inlet for the Spalart-Allmaras turbulence model using second-order central discretization.

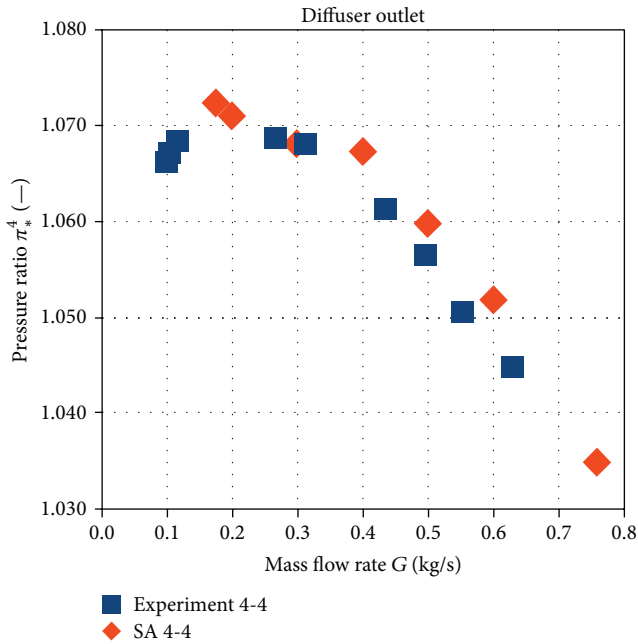


FIGURE 8: Pressure characteristic at the diffuser outlet for the Spalart-Allmaras turbulence model using second-order central discretization.

To provide accurate results, the dependence of mass flow rate in the inlet on the mesh size was investigated (Figure 17). Regime 7 was taken for mesh sensitivity analysis. The coarse meshes consist of $0.3 \cdot 10^5$ and $0.75 \cdot 10^5$ elements; the fine mesh considers $3.9 \cdot 10^5$ elements and the refined mesh $6.12 \cdot 10^5$ elements.

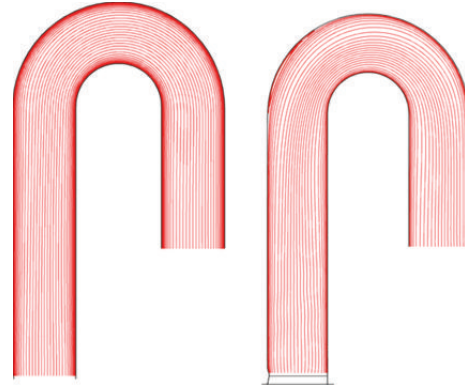


FIGURE 9: Flows paths at mass flow 0.4 kg/s, first-order upwind and second-order central discretization.

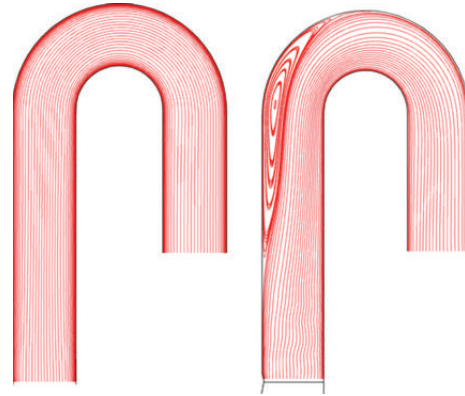


FIGURE 10: Flows paths at mass flow 0.3 kg/s, first-order upwind and second-order central discretization.

TABLE 3: Results of mass flow rate in the inlet for unsteady simulations.

G_{exp}	G_{CM}	Err _{CM}	G_{RM}	Err _{RM}
0.4338	0.4678	7.32	0.4434	3.15
0.3123	0.3443	9.29	0.3264	4.32
0.2661	0.3169	16.03	0.2983	10.79
0.1158	0.2618	55.57	0.2248	48.49

Table 3 presents the results of mass flow rate in the inlet for unsteady simulations for different regimes. Here, G_{exp} is mass flow rate in the inlet taken from the experiments, G_{CM} and G_{RM} are mass flow rates in the inlet for simulation with coarse and refined meshes, and Err_{CM} and Err_{RM} are errors between the experiments and simulation results for coarse and refined meshes. It can be noticed that the difference of the results between coarse and refined meshes is large. The errors differ by 6% for each regime approximately.

Unfortunately, no vortex structures are present and no rotating stall is reproduced for this case. The possible meaning is that the unsteady calculations do not cover nonstationary effects. It could be attributed to one-period geometry or the turbulence model. Further study of this phenomenon is necessary.

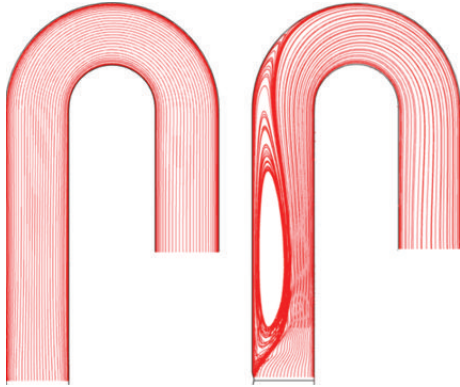


FIGURE 11: Flows paths at mass flow 0.2 kg/s, first-order upwind and second-order central discretization.

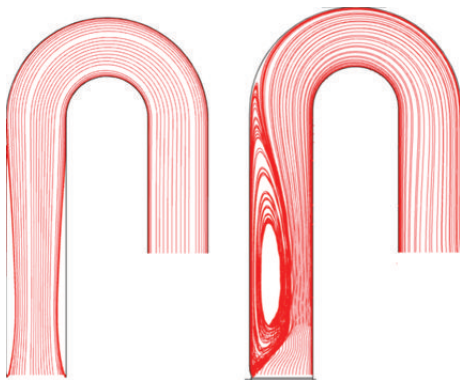
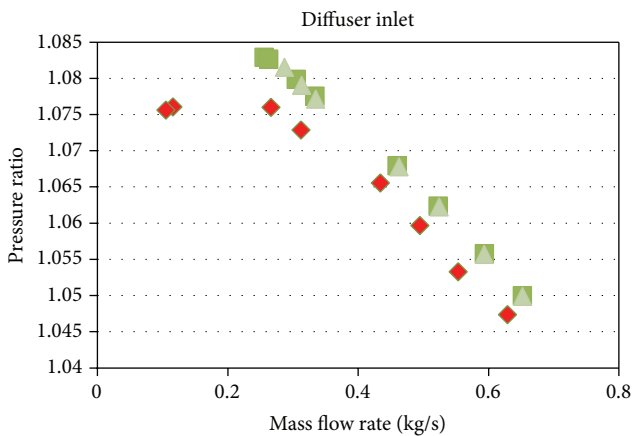


FIGURE 12: Flows paths at mass flow 0.175 kg/s, first-order upwind and second-order central discretization.



- ◆ Experiment
- Coarse mesh
- ▲ Refined mesh

FIGURE 13: Pressure characteristic at the diffuser inlet for the stationary case in the diffuser inlet.

4. Conclusion

Numerical results of executed calculations show strong dependence on the order of discretization. First-order discretization schemes are unacceptable because they do not reproduce large scale vortex structures due to numerical

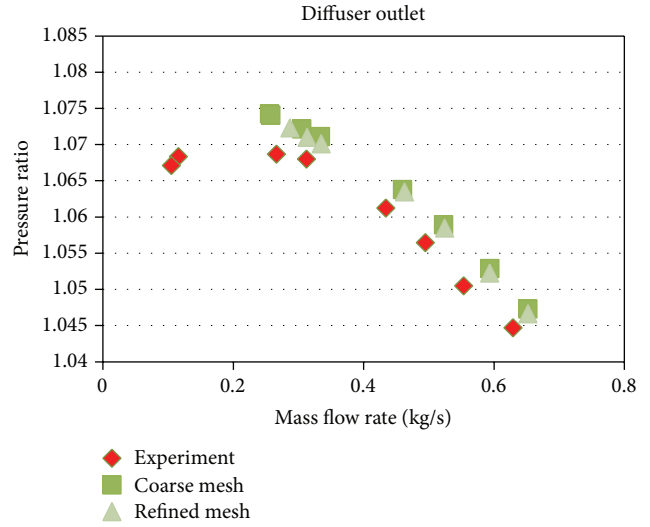


FIGURE 14: Pressure characteristic at the diffuser outlet for the stationary case in the diffuser outlet.

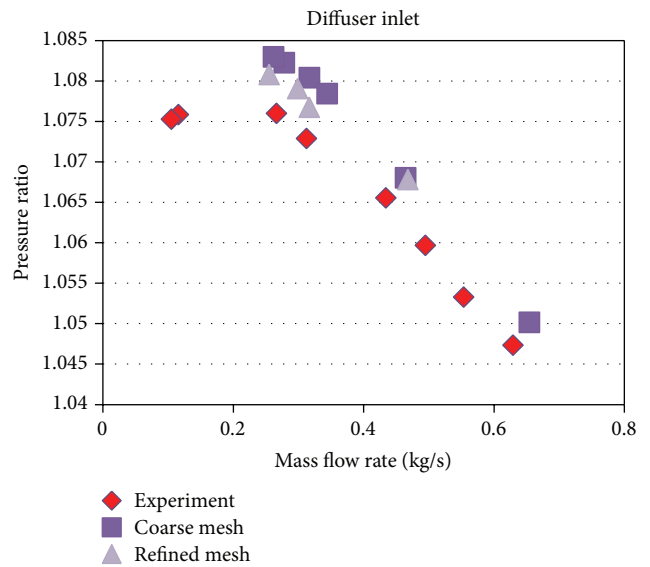


FIGURE 15: Pressure characteristic at the diffuser inlet for the unsteady case in the diffuser inlet.

dissipation effects. Second-order schemes are capable of reproducing these structures.

Numerical results agree with the experiments for regimes with high mass flow rates. In the regimes with low mass flow rates, formation of large nonstationary vortex structure (rotating stall) leads to the inability of stationary models to accurately reproduce flow physics. However, these effects have not been reproduced in unsteady simulations in ANSYS FLUENT 13.0. A possible reason for this is that one-period geometry is incapable of reproducing these nonstationary effects.

Steady-state calculations of a one-period model are required to be done for different turbulence models with second-order discretization schemes and on more refined

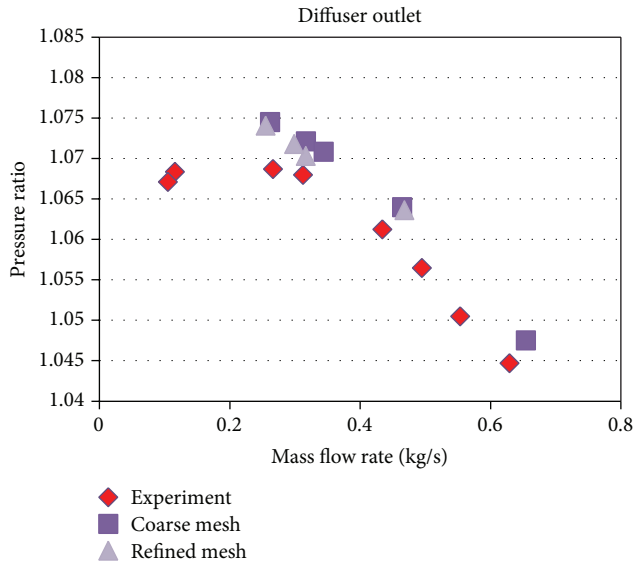


FIGURE 16: Pressure characteristic at the diffuser outlet for the unsteady case in the diffuser outlet.

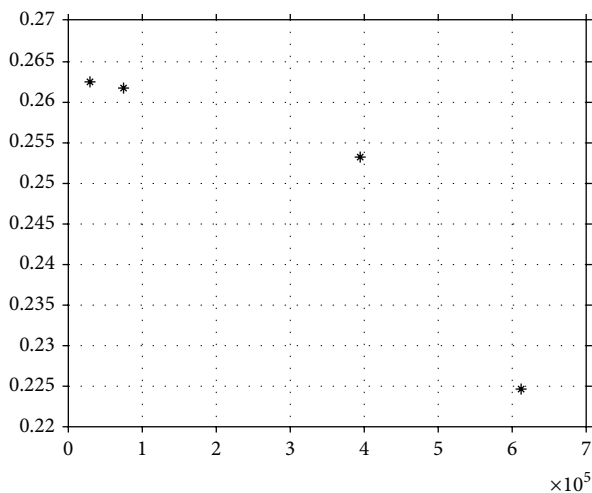


FIGURE 17: Mesh sensitivity analysis.

meshes. Also, unsteady flow simulations for 360-degree geometry should be carried out.

Since the experimental measurements exist for the modelled compressors, it was possible to carry out the verification and validation of user software. The agreement between the results obtained by numerical modelling and by experiments is satisfactory, which enables complete replacement of the time-consuming experimental investigations by much rapid numerical simulations.

The represented numerical modelling of flow in centrifugal compressor makes it possible to carry out the optimisation of basic part of compressor (e.g., impeller) with the aim of improving the efficiency of machinery.

Conflict of Interests

The authors declare that there is no conflict of interests regarding the publication of this paper.

Acknowledgments

The work has been carried out at the Department of Mathematics and Physics, Lappeenranta University of Technology, and Department of Applied Mathematics, Saint Petersburg State Polytechnical University. The experimental results have been obtained by the test stand for gas compressors at the Compressor Design Department, Saint Petersburg State Polytechnical University.

References

- [1] E. Lennemann and J. H. G. Howard, "Unsteady flow phenomena in rotating centrifugal impeller passages," *Journal of Engineering for Gas Turbines and Power*, vol. 92, no. 1, pp. 65–71, 1970.
- [2] D. Eckardt, "Detailed flow investigations within a high-speed centrifugal compressor impeller," *Journal of Fluids Engineering*, vol. 98, no. 3, pp. 390–399, 1976.
- [3] M. V. Casey, P. Dalbert, and P. Roth, "The use of 3D viscous flow calculations in the design and analysis of industrial centrifugal compressors," *Journal of Turbomachinery*, vol. 114, no. 1, pp. 27–37, 1992.
- [4] A. Kosmacheva, *Flow simulation in a gas compressor [M.S. thesis]*, 2011.
- [5] J. A. Bourgeois, *Numerical mixing plane studies with validation for aero-engine centrifugal compressor design [M.S. thesis]*, 2008.
- [6] J. Li, Y. Yin, S. Li, and J. Zhang, "Numerical simulation investigation on centrifugal compressor performance of turbocharger," *Journal of Mechanical Science and Technology*, vol. 27, no. 6, pp. 1597–1601, 2013.
- [7] Z. Guzović, M. Baburić, and D. Matijašević, "Comparison of flow characteristics of centrifugal compressors by numerical modelling of flow," *Journal of Mechanical Engineering*, vol. 51, no. 7-8, pp. 509–518, 2005.
- [8] H.-S. Im, X. Chen, and G.-C. Zha, "Detached eddy simulation of unsteady stall flows of a full annulus transonic rotor," in *Proceedings of the ASME Turbo Expo 2010: Power for Land, Sea, and Air*, pp. 2627–2642, Glasgow, UK, June 2010.
- [9] S. Ljevar, H. C. de Lange, and A. A. van Steenhoven, "Two-dimensional rotating stall analysis in a wide vaneless diffuser," *International Journal of Rotating Machinery*, vol. 2006, Article ID 56420, 11 pages, 2006.
- [10] FLUENT 6.3 User's Guide, 7.13.1, 7.15.1–7.15.3.